



## Optimization of an InGaAsP Vertical-Cavity Surface-Emitting Diode Lasers for High-Power Single-Mode Operation in 1550 nm Optical-Fibre Communication Systems

SAEID MARJANI

Young Researchers Club, Arak Branch, Islamic Azad University, Arak, Iran

Corresponding author: E-mail: saeidmarjani@yahoo.com

(Received: 22 January 2012;

Accepted: 4 February 2013)

AJC-12915

Performance of InGaAsP vertical-cavity surface-emitting diode lasers (VCSELs) at higher powers for second-generation optical-fibre communication systems is investigated with the aid of the comprehensive threshold fully self-consistent optical-electrical-thermal-gain model. The optical confinement introduced by the oxide aperture or a single defect photonic crystal design with holes etched throughout the whole structure, are compared with previous work. Photonic crystal vertical-cavity surface-emitting diode laser shows 30.86 % and 57.02 % lower threshold current than that of the similar oxide confined vertical-cavity surface-emitting diode laser and previous results, respectively. In this way, the minimal threshold power decreases 48.82 % from 1.1176e-5 W to 0.5719e-5 W. This paper provides key results of the threshold characteristics, including the threshold current, the threshold power and the threshold temperature.

**Key Words:** Optimization, InGaAsP, Optical-fibre communication, Diode lasers.

### INTRODUCTION

A crystal is a periodic arrangement of atoms or molecules. The pattern which the atoms or molecules are repeated in space is the crystal lattice. The crystal presents a periodical potential to an electron propagating through it and both the constituents of the crystal and the geometry of the lattice dictate the conduction properties of the crystal. If the dielectric constants of the materials in the crystal are sufficiently different and if the absorption of light by the materials is minimum, then the refractions and reflections of light from all the different interfaces can present many of the same phenomena for photons that the atomic potential produces for electrons.

In recent years, the vertical cavity surface emitting lasers (VCSELs) have attracted researchers<sup>1</sup>. Vertical cavity surface emitting laser is one of the key light sources used in high performance optical communication systems where single mode operation, high output power, high speed modulation and low manufacturing cost are necessary<sup>2</sup>. High optical gain in the active area, high temperature, low threshold current and high thermal conductivity in the reflecting mirrors are the main difficulties in developing VCSELs which are used in the field of optical spectroscopy<sup>3</sup>.

Recently, we proposed a structure for decreasing the threshold current of VCSELs<sup>4</sup> and showed proposed structure decreases the threshold current about 76.52 % from 2.3 mA

to 0.6 mA. There have been a number of reports on the effect of the photonic crystal confined on the modal characteristics by Czyszanowski's group<sup>5-7</sup>. However, the structures presented are different laser wavelength (1.3  $\mu\text{m}$ ), the etching depth and simulation method (the plane-wave admittance method).

In this paper, the impact of the photonic crystal confined and oxide confined (OC) optical confinement schemes on the threshold characteristics of single mode 1.55  $\mu\text{m}$  InGaAsP VCSEL design similar to that reported by Faez *et al.*<sup>4</sup> are investigated and compared with previous results<sup>4,6,7</sup>.

### THEORY AND MODEL

In modeling VCSEL, we consider the electrical, optical and thermal interaction during VCSEL performance<sup>8</sup>. Thus base of simulation is to solve Poisson and continuity equations for electrons and holes. Poisson's equation is defined by the eqn. 1<sup>9</sup>:

$$\nabla \cdot (\epsilon \nabla \Psi) = \rho \quad (1)$$

where  $\Psi$  is electrostatic potential,  $\rho$  is local charge density and  $\epsilon$  is local permittivity. The continuity equations of electron and hole are given by eqns. 2 and 3<sup>9</sup>:

$$\frac{dn}{dt} = G_n - R_n + \frac{1}{q} \nabla \cdot j_n \quad (2)$$

$$\frac{dp}{dt} = G_p - R_p + \frac{1}{q} \nabla \cdot j_p \quad (3)$$

where  $n$  and  $p$  are the electron and hole concentration,  $J_n$  and  $J_p$  are the electron and hole current densities,  $G_n$  and  $G_p$  are the generation rates for electrons and holes,  $R_n$  and  $R_p$  are the recombination rates and  $q$  is the magnitude of electron charge.

The fundamental semiconductor eqns. 1-3 are solved self-consistently together with Helmholtz and the photon rate equations. The applied technique for solution of Helmholtz equation is based on effective frequency method<sup>10</sup> which shows accuracy for great portion of preliminary problems. Two-dimensional Helmholtz equation is solved to determine the transverse optical field profile and it is given by eqn. 4<sup>9</sup>:

$$\nabla^2 E(r, z, \varphi) + \frac{\omega_0}{c^2} \epsilon(r, z, \varphi, \omega) E(r, z, \varphi) = 0 \quad (4)$$

where  $\omega$  is the frequency,  $\epsilon(r, z, \varphi, \omega)$  is the complex dielectric permittivity,  $E(r, z, \varphi)$  is the optical electric field and  $c$  is the speed of light in vacuum. The light power equation relates electrical and optical models. The photon rate equation is given by eqn. 5<sup>9</sup>:

$$\frac{dS_m}{dt} = \left( \frac{c}{N_{\text{eff}}} G_m - \frac{1}{\tau_{\text{phm}}} - \frac{cL}{N_{\text{eff}}} \right) S_m + R_{\text{spm}} \quad (5)$$

where  $S_m$  is the photon number,  $G_m$  is the modal gain,  $R_{\text{spm}}$  is the modal spontaneous emission rate,  $L$  represents the losses in the laser,  $N_{\text{eff}}$  is the group effective refractive index,  $\tau_{\text{phm}}$  is the modal photon lifetime and  $c$  is the speed of light in vacuum. The heat flow equation has the form (eqn. 6)<sup>9</sup>:

$$C \frac{\partial T_L}{\partial t} = \nabla \cdot (\kappa \nabla T_L) + H \quad (6)$$

where  $C$  is the heat capacitance per unit volume,  $\kappa$  is the thermal conductivity,  $H$  is the generation,  $T_L$  is the local lattice temperature and  $H$  is the heat generation term.

Eqns. 1-6 provide an approach that can account for the mutual dependence of electrical, thermal, optical and elements of heat sources. In this paper, we employ numerical-based simulation software to assist in the device design and optimization<sup>9</sup>.

The analyzed structure is similar to the one recently reported by Faez *et al.*<sup>4</sup> has been chosen as a model structure for the analysis of the 1.55  $\mu\text{m}$  InGaAsP VCSEL. The active region consists of six quantum wells where the well is 5.5 nm  $\text{In}_{0.76}\text{Ga}_{0.24}\text{As}_{0.82}\text{P}_{0.18}$  and the barrier is 8 nm  $\text{In}_{0.48}\text{Ga}_{0.52}\text{As}_{0.82}\text{P}_{0.18}$ . In both sides of this active region, there is InP and on top of it, GaAs. The top mirror is 30 layers of GaAs/Al<sub>0.33</sub>Ga<sub>0.67</sub>As with index of refraction 3.38 and 3.05 respectively and the bottom mirror has 28 layers of GaAs/AlAs with index of refraction 3.38 and 2.89, respectively. In the OC VCSEL, the incorporation of a high aluminum content layer (Al<sub>0.98</sub>Ga<sub>0.02</sub>As) in two DBR periods above the active region allows for selective oxidation<sup>11</sup>. Fig. 1(a) shows the photonic crystal VCSEL structure, which is similar to the above VCSEL<sup>4</sup> but made additionally with a single defect photonic crystal etched throughout the whole structure. The optical confinement is achieved by means of seven air holes where the center is missed off to make the defect region, as shown in Fig. 1(b). The crucial photonic crystal parameters are connected by the air hole diameter ( $a$ ), the pitch ( $b$ ) and the optical aperture diameter ( $r$ ), are defined

in Fig. 1(b). The transverse index guiding around the single defect region can be controlled by the air hole diameter the pitch ratio ( $a/b$ ). We fixed the optical aperture diameter at 2  $\mu\text{m}$  and  $a/b$  ratio is varied from 0 to 0.95 for the study.

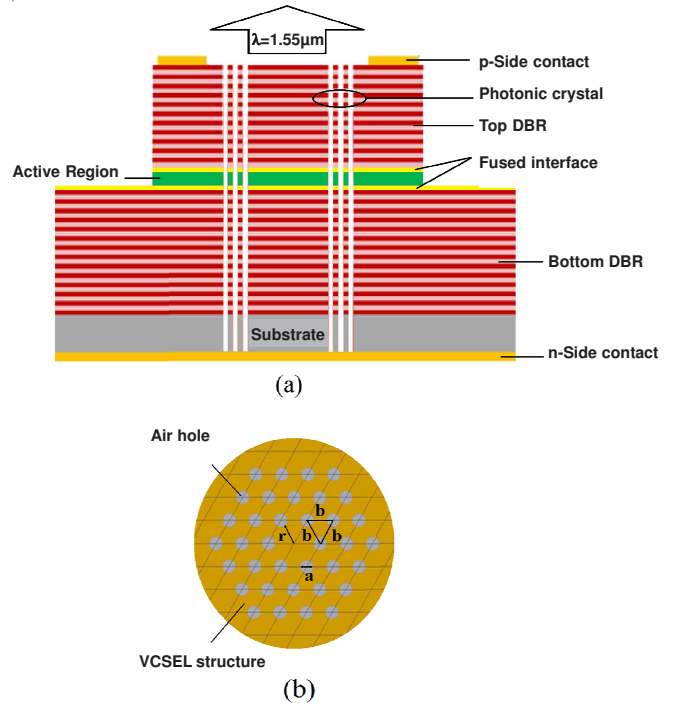


Fig. 1. (a) Schematic structure of the VCSEL device and (b) top view of the triangular-lattice air holes pattern

## RESULTS AND DISCUSSION

The present work allows for determination of the optimum VCSEL structure that is found by a minimization of the threshold power and current with the aid of the comprehensive threshold fully self-consistent optoelectrical-thermal-gain model. A comparison of the threshold characteristics of OC, photonic crystal VCSELs and previous work<sup>4,6,7</sup> as a function of the  $a/b$  ratio is presented in Fig. 2. As can be seen from Fig. 2(a), the logarithmically scaled threshold power of photonic crystal VCSELs decrease gradually with the increase in the  $a/b$  ratio. This initial decrement (from  $a/b = 0$  to  $a/b = 0.9$ ) should be mainly due to improving the optical confinement by the photonic crystal. For  $a/b = 0.9$  the threshold power reaches a minimum value of  $0.5719 \times 10^{-5}$  W and then rapidly increases for  $a/b = 0.95$ , which should be mainly due to blocking of most of the current flow by the holes. The minimal threshold power is lowered by 48.82 % from  $1.1176 \times 10^{-5}$  W to  $0.5719 \times 10^{-5}$  W than that of the OC VCSEL, since, the electrical resistance of the etched photonic crystal regions is increased.

Fig. 2(b) shows a monotonic decrease in the logarithmically scaled threshold current of photonic crystal VCSELs with the increase in the  $a/b$  ratio. This is caused by more effective optical confinement and stronger limitation of the current flow to the active region. As shown in Fig. 2(b), Photonic crystal VCSEL shows 30.86 % and 57.02 % lower threshold current than that of the similar oxide confined VCSEL and previous results<sup>4</sup>, respectively. Threshold current for two photonic crystal VCSEL structures<sup>6,7</sup> determined by  $r = 4 \mu\text{m}$ ,  $a/b = 0.5$

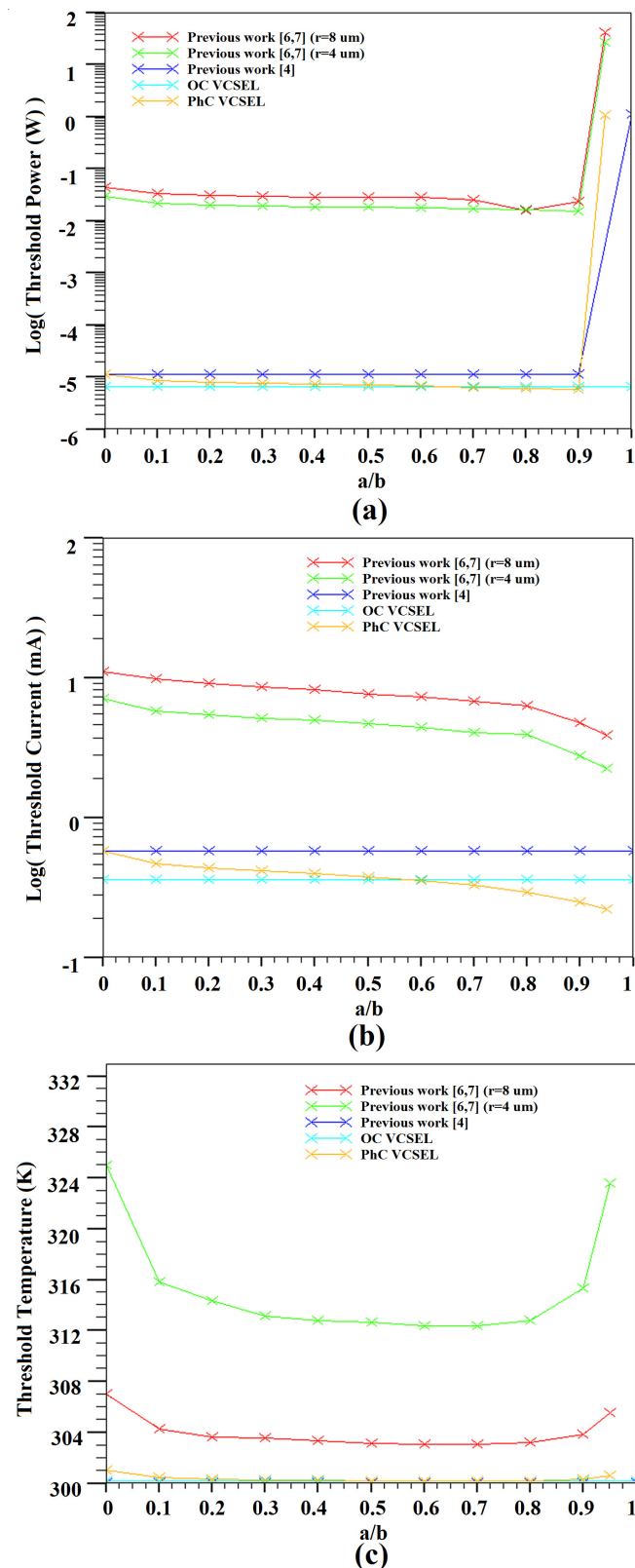


Fig. 2. Threshold characteristics of OC, photonic crystal VCSELs and previous work<sup>4,6,7</sup> as a function of the  $a/b$  ratio

and  $r = 8 \mu\text{m}$ ,  $a/b = 0.5$  are 4.9 mA and 7.11 mA, respectively, which are very close to previous values of 4.89 mA and 7.12 mA, respectively<sup>7</sup>. We fixed the depth of the photonic crystal holes at  $7 \mu\text{m}$  for two photonic crystal VCSEL structures.

Fig. 2(c) shows a threshold temperature increase for  $a/b = 0$  than that of the OC VCSEL, since, the thermal focusing is the unique waveguiding mechanism induced by the photonic crystal structure. As can be seen from Fig. 2(c), threshold temperature of the OC VCSEL is always smaller than that of the photonic crystal VCSEL. This is caused by the more efficient heat sinking process in the OC VCSEL. For  $a/b = 0.7$  the threshold temperature reaches a minimum value of 300.147 K that is the optimum configuration for over threshold operation.

## Conclusion

This article described the threshold characteristics of a Single Mode  $1.55 \mu\text{m}$  InGaAsP vertical cavity surface emitting laser with two different optical confinement structures and compared with previous work. The results indicate that lowest threshold current and threshold power for  $a/b = 0.9$  that shows 30.86 % and 57.02 % lower threshold current than that of the similar oxide confined VCSEL and previous results, respectively. Also, the minimal threshold power decreases 48.82 % from  $1.1176 \times 10^{-5} \text{ W}$  to  $0.5719 \times 10^{-5} \text{ W}$ .

## REFERENCES

1. K. Iga, *J. IEEE Select. Topics Electron*, **16**, 1201 (2000).
2. M. Dems, R. Kotynski and K. Panajotov, *J. Opt. Express*, **13**, 3196 (2005).
3. E. Kapon and A. Sirbu, *J. Nature Photonics*, **3**, 27 (2009).
4. R. Faez, A. Marjani and S. Marjani, *J. IEICE Electron. Express*, **8**, 1096 (2011).
5. T. Czystanowski, M. Dems, R. Sarzala, W. Nakwaski and K. Panajotov, *J. IEEE Quantum Electron.*, **47**, 1291 (2011).
6. T. Czystanowski, M. Dems, H. Thienpont and K. Panajotov, *J. Phys. D: Appl. Phys.*, **41**, 085102 (2008).
7. T. Czystanowski, IEEE/LEOS Winter Topicals Meeting Series, Innsbruck, Vol. 20, pp. 20-21 (2009).
8. P.S. Menon, K. Kumarajah, M. Ismail, B.Y.M. Majlis and S. Shaari, *J. Opt. Commun.*, **31**, 81 (2010).
9. SILVACO International, ATLAS User's Manual, USA, SILVACO International Incorporated (2010).
10. H. Wenzel and H.J. Wunsche, *IEEE J. Quantum Electron.*, **33**, 1156 (1997).
11. K.D. Choquette, K.M. Geib, C.I. Ashby, R.D. Twisten, O. Blum, H.Q. Hou, D.M. Follstaedt, B.E. Hammons, D. Mathes and R. Hull, *IEEE J. Sel. Topics Quantum Electron.*, **3**, 916 (1997).